

Micellization of Sliding Polymer Surfactants

Vladimir A. Baulin¹, N.-K. Lee², Albert Johner^{1,3} and Carlos M. Marques^{1,*}

¹*Institut Charles Sadron, CNRS UPR 22, 67083 Strasbourg Cedex, France.*

²*Department of Physics, Sejong University, Seoul 143-743, South Korea.*

³*also LEA ICS/MPIP, Ackermannweg 10, 55128 Mainz, Germany.*

Following up a recent paper on grafted sliding polymer layers (*Macromolecules* **2005**, *38*, 1434-1441), we investigated the influence of the sliding degree of freedom on the self-assembly of sliding polymeric surfactants that can be obtained by complexation of polymers with cyclodextrins. In contrast to the micelles of quenched block copolymer surfactants, the free energy of micelles of sliding surfactants can have two minima: the first corresponding to small micelles with symmetric arm lengths, and the second corresponding to large micelles with asymmetric arm lengths. The relative sizes and concentrations of small and large micelles in the solution depend on the molecular parameters of the system. The appearance of small micelles drastically reduces the kinetic barrier signifying the fast formation of equilibrium micelles.

1. INTRODUCTION

Predicting, controlling and finely tuning the self-assembly properties of amphiphiles through molecular design is a problem of central importance in physical chemistry.^{1,2} It is arguably also one of its major contributions to other fields: in the biological realm, where self-assembled phospholipids build the walls of liposomes and cells; in cosmetics, pharmaceuticals or detergency, where many formulations are self-assembled solutions of surfactants, phospholipids and other amphiphile molecules. In this context, diblock copolymers have emerged as a paradigm for self-assembly.^{3,4,5,6} Typically, the insoluble block drives the chains to self-associate and the compositional asymmetry between the soluble and insoluble blocks defines the assembling geometry.⁵ The many possibilities for architecture building offered by polymer synthesis and the development of polymer theory led to an unprecedented power of molecular control over the self-assembling structures of these so called macrosurfactants. It is nowadays possible, for instance, to build different self-assembled structures from diblock, triblocks and many other block copolymers, to introduce charges at different places along the chains with single charge accuracy, to form reversible or frozen structures, to combine flexible and semi-flexible blocks, *etc.* However, a major difficulty still hinders progresses in the predictive power of micellization theories. Indeed, the macromolecular character of such surfactants implies that there is a large kinetic barrier for micelle formation, and the thermodynamic predictions for typical quantities such as the critical micellar concentration or the aggregation number are in many cases only marginally relevant. In this paper we discuss a novel macrosurfactant architecture, based on rotaxane inclusion complexes,⁷ that can lead to a significant decrease of the kinetic barrier to micellization.

Rotaxanes are molecular complexes formed when a ring like molecule, the rotor, is threaded over a linear molecule, the rotating axis.⁷ Unthreading of the ring can be prevented by subsequent capping of the axis ends.^{8,9}

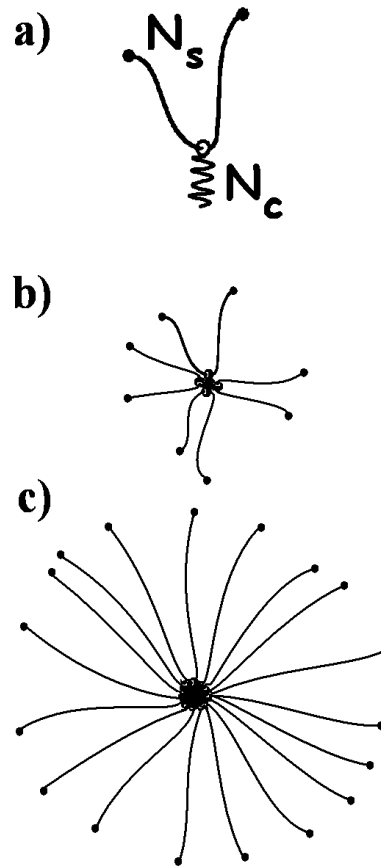


FIG. 1: Schematic representation of sliding a) unimers comprised of soluble insoluble blocks of lengths N_s and N_c , respectively, b) small symmetric micelles and c) big asymmetric micelles.

Rotaxanes can be made by combining different linear polymers^{10,11} with different cyclic molecules, in several solvents.¹² One of the most well studied systems involve poly(ethylene-oxide) and α -cyclodextrins, which are oligosaccharides of 6 glucose units assembled as rings. When an inclusion complex formed by one α -cyclodextrin

and one PEO chain is attached to a surface by grafting the α -CD, it results a novel structure of polymer layers for which we recently¹³ coined the acronym SGP layers, for sliding grafted polymer layers. Contrary to the usual end-grafted polymer layer, in the SGP layers the chains retain the ability to slide through the grafting ring, a new degree of freedom that allows, as we recently have shown, to better relax the layer structure. In particular, our work suggests that in spherical, star-like layers, as obtained for instance if one attaches the α -CD ring to a small colloid, sliding of the polymers through the ring entails a truly versatile polymer layer structure. At low number of grafts the chains adopt mostly symmetric configurations with two comparable arm-sizes whereas with many grafts the adopted configurations are asymmetric with essentially one long arm participating in the corona. It was also shown that there exists an intermediate range of grafting numbers where the number of arms participating in the corona is constant and where the addition of more grafts leads to the progressive replacement of symmetric configurations by twice as much asymmetric ones. Conversely, in flat dense SGP layers, chains adopt only asymmetric configurations, having hence the same structure as the quenched ones. An important consequence for self assembly is that the free energy of the curved SGP layers has a different structure from the usual polymer layers grafted to spherical surfaces, but that the free energy of flat SGP layers only marginally differs from their non-sliding equivalents.

We consider the micellization of decorated “one-pearl necklaces” where the driving force for self-assembly is provided by the bead decoration, an insoluble chain chemically attached to the ring molecule (see Figure 1). The consequences of the sliding degree of freedom on the self-assembly of sliding polymeric surfactants are discussed by focusing on curved self-assembled structures, since for flat self-assembled layers only marginal differences are expected with the usual grafted layers. After a short reminder on diblock-copolymer micellization, we recall the theoretical description of the spherical SGP layer, before a detailed discussion of the possible micellization scenarios for this new family of macrosurfactant architectures (Figure 1).

2. MICELLIZATION OF DIBLOCK-COPOLYMERS

In this section we briefly discuss the theory of micellization of block copolymers, see *e.g.* Ref. 14. Consider a solution of monodisperse block copolymer with N_c insoluble and N_s soluble units. The insoluble blocks tend to aggregate and favor large aggregates while coronas of soluble blocks oppose the formation of big micelles. The free energy per unit volume F , of the solution of non-interacting micelles is a sum running over the aggregation

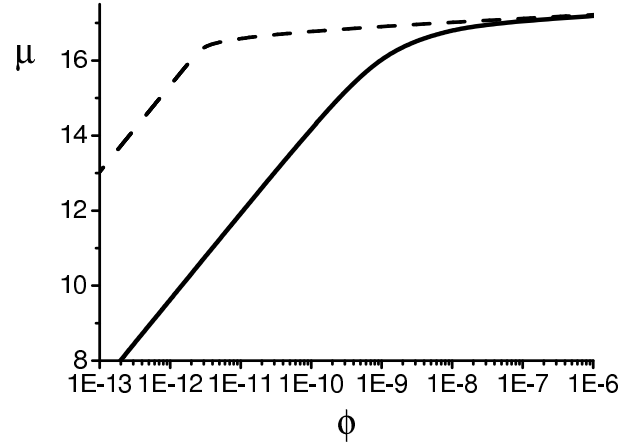


FIG. 2: Chemical potential μ as a function of total concentration for quenched (dashed line) and sliding (solid line) micelles. Parameters used: $N_S = 300$, $N_c = 62$ and $\sigma = 0.5$.

number p :

$$F = \sum_{p=1}^{\infty} c_p \left[k_B T \ln \left(\frac{c_p}{e} N_T b^3 \right) + F_p \right] \quad (1)$$

where F_p and c_p is the free energy and the number density of a micelle comprising p surfactant chains respectively. The multiplier $N_T b^3$ with $N_T = N_c + N_s$ being the total volume of a copolymer.¹⁵ This multiplier was often overlooked, a general discussion is provided by Riess,¹⁶ who gives the relevant elementary volume, in our case $N_T b^3$, for microemulsions, assemblies of droplets, etc. The equilibrium distribution of chains in micelles is obtained by minimizing F with respect to c_p along with the mass conservation constraint:

$$\sum_{p=1}^{\infty} p c_p = \phi \quad (2)$$

where ϕ is the total number of chains per unit volume. This gives the equilibrium densities of p -arm micelles in the form $c_p b^3 N_T = \exp \{(\mu p - F_p)/k_B T\}$, where:

$$\mu = F_1 + k_B T \ln(c_1 N_T b^3) \quad (3)$$

is the chemical potential of unimers.

Thus we can rewrite the equilibrium c_p as

$$c_p = \frac{(c_1 N_T b^3)^p}{N_T b^3} \exp \left(-\frac{F_p - p F_1}{k_B T} \right) \quad (4)$$

Rather than the distribution c_p , we will often use the more convenient function $\Omega_p = \ln(c_1/c_p)$:

$$\Omega_p = F_p - p F_1 - (p - 1) k_B T \ln(c_1 N_T b^3) \quad (5)$$

which may be considered as the thermodynamic potential. Given a value of c_1 in eq. 4 allows us to calculate the whole distribution c_p and the corresponding total chain concentration ϕ . Experimentally, the chemical

potential μ is often studied as a function of ϕ . We obtained the chemical potential curve from eqs.(2)-(4) with c_1 as the parameter. A kink in the representation (Figure 2, dashed line) is commonly used as an indicator for the onset of micellization. Usually only a narrow range of unimer concentrations at equilibrium c_1 falls in the physically acceptable condition: $N_T\phi b^3 \ll 1$. When no interaction between micelles is accounted for, the more stringent criterion $\sum_p c_p V_p < 1$ should be obeyed where V_p is the volume of a micelle comprising p surfactants.

The micellization scenario depends on the precise form of the free energy F_p , discussed in the following paragraphs for quenched copolymers and annealed sliding copolymers.

3. FREE ENERGY OF STAR-LIKE MICELLES

The free energy of a micelle contains the molecular characteristics of the micellization process. Thus, in order to investigate the micellization of sliding polymer surfactants, we have to specify the explicit form for the corresponding F_p . The free energy of a micelle is the sum of the core and of the corona contributions. Hereafter energies are expressed in $k_B T$ units.

3.1. Core contribution

We assume that the insoluble blocks form a dense homogeneous core where soluble blocks and the solvent cannot penetrate. Hence the micelle free energy has two core contributions: (i) the surface tension term, $F_c = 4\pi\sigma R_c^2$, where R_c is the radius of the core and σ is the core-solvent surface tension expressed in $k_B T/b^2$ units. For an incompressible core of size $R_c = (3/(4\pi)pN_c)^{1/3}b$, this leads to $F_c = c\sigma N_c^{2/3} p^{2/3}$, where $c = (36\pi)^{1/3}$. (ii) Gaussian elastic contributions arising from stretching of the insoluble blocks in the core, $F_{el} = wpR_c^2/(N_c a^2) = wp^{5/3}/N_c^{1/3}$, where $w = 3\pi^2/80$ reflects the spherical geometry of the core. The value of w is obtained from SCF theory in the strong stretching limit.¹⁷ Although the elastic contribution of the core is only larger than $k_B T$ for micelles with large cores, we keep it for convenience.¹⁸

3.2. Corona contribution

For large soluble blocks, as considered here, the corona is usually envisioned as a star of soluble blocks radially stretched away from the spherical core. The partition function Z_p of a star with p equal arms of contour length N_s is given by the critical exponent γ_p , $Z_p \sim N_s^{\gamma_p - 1}$.¹⁹ Star exponents γ_p are known exactly in two dimensions and for ideal chains ($d \geq 4$). In three dimensions ϵ -

expansions ($\epsilon = 4 - d$) are available, to first order:¹⁹

$$\gamma_p - 1 = -\frac{\epsilon}{16}p(p - 3) + o(\epsilon^2) \quad (6)$$

Recently Monte Carlo simulations were carried out by Hsu *et al.*²⁰ in order to find the exact values of γ_p for a large range of p values. The results do not quantitatively agree with the classical predictions of the Daoud-Cotton model²¹ $\gamma_p - 1 \sim -p^{3/2} + \dots$, indicating that the asymptotic limit of very large p numbers, where subdominant powers of p are negligible, is not yet reached. If we insist on fitting Hsu *et. al.* results to the Daoud and Cotton model, say between $p = 20$ and $p = 60$, where the simulated arms are still fairly long, the obtained amplitude is close to 0.2. It seems that the asymptotic limit, restricted to the leading term, is also out of experimental reach. Authors showed that the best fit of the simulation data with a power law $\sim -p^z$ is obtained with $z = 1.68$. Our discussion below is based on the simulation data and we will use, for convenience, the fitting function of the form close to eq. (6): $-p(bp - a)^z/16$ reflecting the simulation results. The best fit is

$$\gamma_p - 1 = -\frac{p}{16} (1.5p - 6)^{0.7}, \quad p > 4 \quad (7)$$

while for $p < 4$ we take values from the table of Ref. 20.

When there is sliding degree of freedom, the free energy of the corona has a more complex structure. The possibility for the soluble blocks to slide through a ring results in an annealed arm length distribution in the coronas of such micelles made of p -chains. Adjusting the length of the arm in the corona can decrease the crowding effect originating from the steric repulsions between soluble blocks. In our previous paper¹³ we found three possible regimes for the sliding coronas depending on the number of sliding chains per aggregate. The transition between these regimes is determined from a threshold value of the number of arms p^* , defined by the conditions $\gamma_{p^*} - \gamma_{p^*-1} > -1$ and $\gamma_{p^*+1} - \gamma_{p^*} \leq -1$. If the number of chains per aggregate is small, $p \leq p^*/2$, the corona is fully annealed and the sliding chains are likely to adopt any configuration. We call such micelles symmetric micelles, since symmetric configurations are prevalent. The corona properties are determined by configurations with $2p$ arms and its partition function is given by¹³

$$Z_p \propto N_s^p N_s^{\gamma_{2p}-1}, \quad p \leq p^*/2 \quad (8)$$

For a larger number of grafting chains, in the intermediate regime, $p^*/2 < p < p^*$, only $p^* - p$ chains adopt symmetric configurations, while the rest of the chains are stretched out from the ring. The corona has p^* arms and its partition function reads

$$Z_p \propto N_s^{p^*-p} N_s^{\gamma_{p^*}-1}, \quad p^*/2 < p < p^* \quad (9)$$

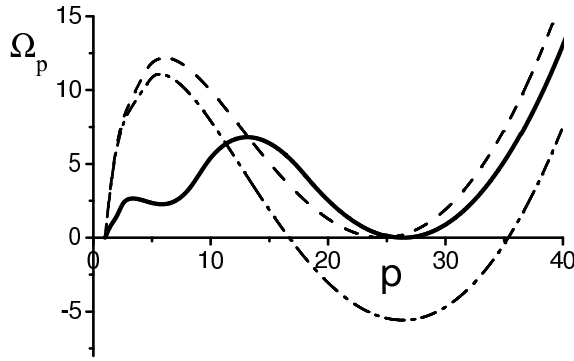


FIG. 3: Potential $\Omega_p = \ln(c_1/c_p)$ as a function of the aggregation number p for sliding micelles (solid line, total surfactant concentration $\phi = 3 \times 10^{-8}$) and for quenched micelles (dashed line, $\phi = 1 \times 10^{-10}$, dash-dotted line, $\phi = 3 \times 10^{-8}$, same as for sliding micelles) for the set of parameters: $N_s = 300$, $N_c = 70$ and $\sigma = 0.5$. Micelles form almost without kinetic barrier from sliding polymer surfactants.

For even larger micelles, $p \geq p^*$, all the chains in the corona are strongly asymmetric and the partition function of the corona coincide with the partition function of a quenched star:

$$Z_p \propto N_s^{\gamma_p - 1}, \quad p \geq p^* \quad (10)$$

The determination of the threshold value of the number of arms p^* strongly depends on our knowledge of the values of the critical exponents γ_p . Our previous estimates¹³ were based on the first order ϵ -expansion (Eq. 6) yielding $p^* = 9$. However, if we use the values obtained from the computer simulations in ref. 20, we get $p^* = 18$. Thus, in the following we assume the latter estimate as most accurate. We use our fitting function (7) for the values of γ_p , and the free energy of the sliding corona of a micelle $F_p^{corona} = -\ln Z_p$ is determined as a piecewise function of the number of chains p .

3.3. Total free energy

Combining all terms together, the energy of a micelle is given by

$$F_p = F_p^{corona} + c\sigma N_c^{2/3} p^{2/3} + wp^{5/3}/N_c^{1/3} \quad (11)$$

with

$$F_p^{corona} = f(p) \ln N_s \quad (12)$$

where $f(p)$ is defined piecewise by eqs.(8,9,10) as discussed in the previous section for sliding copolymers whereas for quenched copolymers: $f(p) = -(\gamma_p - 1)$.

Note that the corona free energy of sliding surfactant unimers ($p = 1$) is $F_1^s = -\gamma_1 \ln N_s$ while that of the

quenched unimer is $F_1^q = -(\gamma_1 - 1) \ln N_s$. Thus the free energy of sliding surfactant is about $-\ln N_s$ less than that of quenched ones with the same soluble block size.

Next we use the expressions of the free energy F_p to compute the micelle size distribution for both quenched and sliding copolymers.

4. MICELLE-SIZE-DISTRIBUTION: SLIDING VS. QUENCHED COPOLYMERS

A preferred aggregation number is reflected by a minimum in the potential Ω_p . Roughly speaking, the corresponding aggregates will dominate over unimers if the minimum potential value is negative. For usual quenched copolymers the potential has only one, pretty sharp, minimum (see Figure 3) and the polydispersity of spherical micelles is usually very low, the distribution c_p being sharply peaked around the average aggregation number p_m . In this sense, quenched copolymer association should be termed *closed* association where the distribution is dominated by aggregates of uniform size with weak fluctuations appearing at a well defined unimer concentration. In the common used classification, *open* association means that aggregates of different sizes significantly contribute to the distribution and appear gradually. The practical relevance of this classification has been critically discussed recently.²²

The average aggregation number and the *CMC* are found from the conditions: $\Omega_p = \partial \Omega_p / \partial p = 0$.²³ The minimum is separated from the origin by a kinetic barrier. Thus it takes a typical time $\sim \exp(-U_{\max}/kT)$ for isolated chains to form a micelle; with U_{\max} the maximum of the barrier. A rough scaling estimate gives $U_{\max}/kT \sim \sigma N_c^{6/5}$.²⁴ Depending on the conditions, this time for usual block copolymer micelles can be very large. Very often, quenched copolymer micelles do not form over reasonable time scales at the *CMC*, where they are thermodynamically favored. Only at much higher concentrations, the barrier U_{\max}/kT becomes low (see Figure 3).

In contrast to the quenched case, the potential $\Omega_p = \ln(c_1/c_p)$ (Eq. (5)) for sliding micelles can have two minima. One corresponds to small symmetric micelles with aggregation numbers up to 9, and the second corresponds to big asymmetric micelles (Figure 3). The appearance of small micelles leads to a drastic decrease of the kinetic barrier, such that the first minimum is separated from the origin by a barrier of order kT signifying the fast formation of equilibrium micelles. The chemical potential μ of sliding copolymers as a function of ϕ presents a rounded kink as compared to the quenched case (Figure 2).

Depending on molecular parameters of the system, the formation of small micelles can follow (Figure 4a and 4c) or precede (Figure 4b and 4d) the formation of big micelles. Typical examples of the mass distribution in micelles, pc_p/ϕ , with increasing polymer concentration are

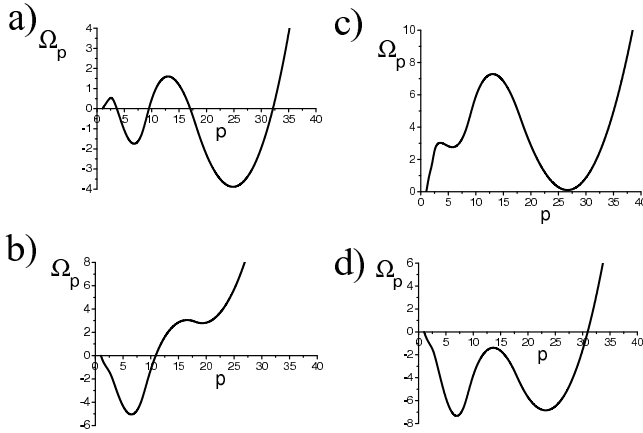


FIG. 4: Typical examples of the potential $\Omega_p = \ln(c_1/c_p)$ for different set of parameters: a) $N_s = 300$, $N_c = 60$, $\sigma = 0.5$, $\phi = 3.3 \times 10^{-5}$, b) $N_s = 300$, $N_c = 55$, $\sigma = 0.6$, $\phi = 2.0 \times 10^{-8}$, c) $N_s = 1000$, $N_c = 60$, $\sigma = 0.5$, $\phi = 2.8 \times 10^{-5}$, d) $N_s = 10000$, $N_c = 60$, $\sigma = 0.7$, $\phi = 7.8 \times 10^{-7}$. Depending on parameters, small micelles appear first, a) and c), or formation of big micelles happens earlier, b) and d).

shown in Figure 5. The equilibrium aggregation number switches between symmetric (small) and asymmetric (big) micelles as the concentration increases. Tuning the parameters of the system, either the surface tension of the core, σ , or the relative length of the blocks (in our case we vary N_c keeping N_s constant), we can change the order of the appearance of small and big micelles. Figure 6 shows the corresponding state diagram which is related to Figure 7. When big and small micelles coexist the big ones usually dominate by mass. Hence we represent the boundary between big and big+small micelles by a dashed line.

Though the full potential (Eq.5) is uneasy to handle analytically, we may somewhat simplify it by omitting the stretching of the insoluble blocks. The aggregation number of a vanishing minimum of this approximate potential (for some chemical potential) is then solution of the following equation:

$$\frac{(p-1)\frac{\partial f(p)}{\partial p} - f(p) + f(1)}{p^{2/3} + 2p^{-1/3} - 3} = \frac{1}{3} \frac{c\sigma N_c^{2/3}}{\ln N_s} \quad (13)$$

the left hand side of this equation $h(p)$ collects all the terms depending on p . Thus, in this approximation the desired aggregation numbers depend only on the combination of parameters $\beta = \frac{1}{3}c\sigma N_c^{2/3} / \ln N_s$. It is easy to see that in the quenched copolymer case there is indeed only one solution of p_m and in the Daoud-Cotton limit $p_m \sim (\sigma N_c^{2/3} / \ln N_s)^{6/5}$, a classical result.

It is worthwhile discussing the number of solutions of eq. (13) as a function of the parameter β for sliding copolymers. It can be obtained by counting the number of intersections of $h(p)$ (Figure 7) with the line parallel

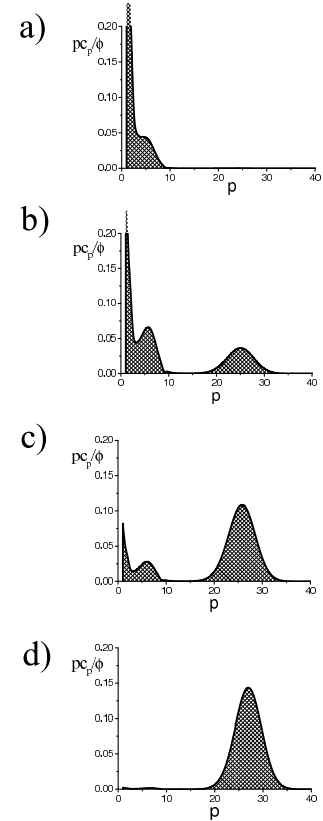


FIG. 5: Evolution of the mass distribution in micelles, pC_p/ϕ , with increasing total concentration ϕ : a) $2. \times 10^{-10}$, b) $5. \times 10^{-10}$, c) $2. \times 10^{-9}$, d) $8. \times 10^{-8}$ for $N_s = 300$, $N_c = 70$ and $\sigma = 0.5$.

to the abscissa. In the first region, $\beta \lesssim 1.38$, there is only one intersection. It corresponds to one minimum in $\Omega_p(p)$. The number of arms p is small, thus this region corresponds to the coexistence of unimers with small symmetric micelles. In the region $1.38 \lesssim \beta \lesssim 2.77$ there are three intersections showing the existence of two minima separated by a barrier. Small micelles with aggregation numbers $p < p^*/2 = 9$ coexist with big micelles with $p > p^* = 18$. In the third regime, $\beta \gtrsim 2.77$, there are only asymmetric micelles of high aggregation numbers. The crossover values of the parameter β are compatible with Figure 6, where the crossover values of N_c are 40 and 93. For given values of parameters (N_c , N_s , σ) it should further be checked that the micelles exist for physical concentrations.

Figure 7 also shows the aggregation number of quenched copolymer micelles as a function of β (dashed line). The difference with large sliding micelles is due to a shift in the free energy of a unimer from F_1^s to F_1^q . The Daoud-Cotton line is also shown (dotted line). As already discussed, no agreement can be obtained using a simple Daoud-Cotton power law.

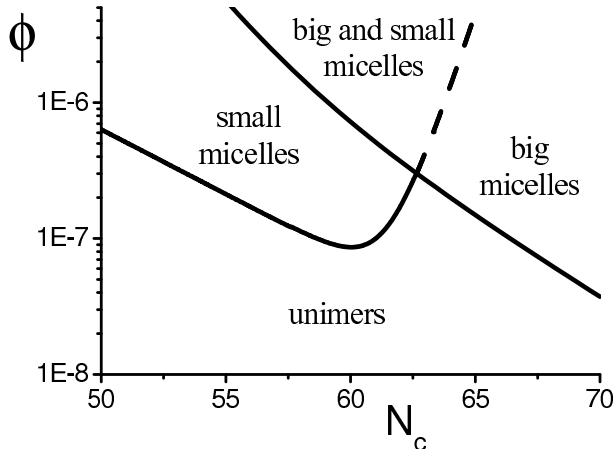


FIG. 6: Schematic diagram of different types of micelles present in a solution. Labels designate regions where the indicated structures are dominant. Parameters used: $N_S = 300$, $\sigma = 0.5$. The boundary between the region of big micelles and the region of the coexistence of small and big micelles is indicated as dashed line, because big micelles usually dominate by mass in both regions.

5. CONCLUDING REMARKS

Sliding-diblock-copolymer surfactants where the soluble and insoluble blocks are topologically tethered by a small ring polymer show a much reacher micellization behavior than the corresponding quenched diblock copolymers. When the size of insoluble blocks is not too long, both small micelles (with an aggregation number slightly smaller than $p^*/2 = 9$) and large micelles (with an aggregation number slightly larger than $p^* = 18$) may coexist in the solution. In the small micelle each copolymer participates in the corona with two arms whereas in the large micelle the asymmetric arm length distribution is dominant. Hence coronas in small and large micelles comprise a similar number of arms. Small micelles can form without appreciable kinetic barrier at the lowest concentration where they are thermodynamically favored. The barrier opposing the formation of the larger micelle remains modest. This is in marked contrast to the corresponding quenched copolymers where kinetic barriers are very high at the same concentrations. Which micelle appears first with increasing concentration depends on the block asymmetry. At somewhat higher concentrations, the micelle-size-distribution broadens and covers the whole range from the small to the large aggregation number described previously.

For large insoluble blocks only the large micelles, similar to the quenched ones, form. Due to the loss of the sliding degree of freedom upon association, the annealed

CMC is higher than the quenched one. On the other hand the kinetic barrier is markedly lower for annealed copolymer micelles (typically by a factor 2) that may form at the CMC within experimental times.

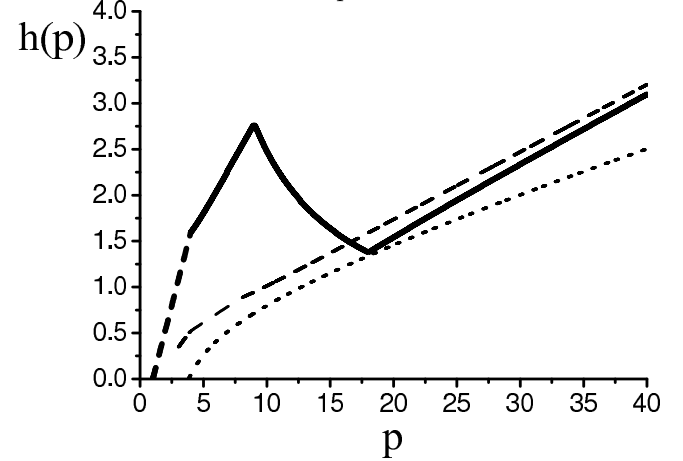


FIG. 7: Graphical solution of the eq. (13). For values of $\beta = \frac{1}{3}\sigma N_c^{2/3} / \ln N_s$ between 1.38 and 2.77 a small symmetric micelle and a large asymmetric one can be more stable with respect to the unimer (for different chemical potentials). The bold dashed line ($p < 3$) was not calculated. The thin dashed line corresponds to quenched copolymers, where there is only one micelle size. The dotted line corresponds to the Daoud-Cotton model for quenched copolymers.

Our description of star-like micelles is based on excellent values of the vertex exponents from a recent simulation by Hsu *et. al.*²⁰ We think that this improves over the standard Daoud and Cotton model for the classic quenched micelles.

Sliding copolymers are a new interesting example of non ionic annealed copolymers. Some charged micelles can also display a similar behavior as reported by Zhulina and Borisov for insoluble/annealed-polyelectrolyte diblocks.²⁵ To our knowledge only flat brushes of complexing polymers have been studied theoretically.²⁶ Diblocks where the soluble block forms a complex with small colloids (proteins) also belong to the class of annealed copolymers. One may speculate whether such diblocks also form two types of micelles.

Acknowledgments

V. B. gratefully acknowledges the French Space Agency, CNES for a research post-doctoral fellowship. N. K. L. acknowledges financial support from KOSEF/CNRS exchange program N18055.

* Electronic address: marques@ics.u-strasbg.fr

¹ Safran S., *Statistical Thermodynamics of Surfaces, Inter-*

faces and Membranes, Addison-Wesley, 1994.

² Israelachvili J. N., *Intermolecular and surface forces*, 2nd ed; Academic Press: Orlando, 1991.

³ Riess, G.; Hurtrez, G.; Bahadur, P. *Block Copolymers*, 2nd ed.; Wiley: New York, 1985; Vol. 2.

⁴ Hamley I.W., *Block Copolymers in Solution : Fundamentals and Applications*, John Wiley & Sons, 2005.

⁵ Alexandridis P., Lindman B., *Amphiphilic Block Copolymers*; Elsevier: Amsterdam, 2000.

⁶ Zhang L., Eisenberg A., *Science*, **1995**, *268*, 1728-1731.

⁷ Nakashima N., Kawabuchi A., Murakami H., *J. Inc. Phen. Mol. Rec. Chem.* **1998**, *32*, 363-373.

⁸ Ogino, H. *J. Am. Chem. Soc.* **1981**, *103*, 1303.

⁹ Ogino, H.; Ohata, K. *Inorg. Chem.* **1984**, *23*, 3312.

¹⁰ Harada, A. *Coord. Chem. Rev.* **1996**, *148*, 115-133.

¹¹ Wei, M.; Shin, I. D.; Urban, B.; Tonelli, A. E. *J. Pol. Sci. Part B: Pol. Phys.* **2004**, *42*, 1369-1378.

¹² Rekharsky, M. V.; Inoue, Y. *Chem. Rev.* **1998**, *98*, 1875-1917.

¹³ Baulin V. A., Johner A., Marques C. M., *Macromolecules*, **2005**, *38*, 1434-1441.

¹⁴ Sens P., Marques C. M., Joanny J.-F., *Macromolecules*, **1996**, *29*, 4880-4890.

¹⁵ Nyrkova I. A., Semenov A. N., *Faraday Discuss.*, **2005**, *128*, 113-127.

¹⁶ Kegel W. K., Reiss H., *Ber. Bunsen-Ges. Phys. Chem.*, **1996**, *100*, 300.

¹⁷ Zhulina E. B., Adam M., LaRue I., Sheiko S. S., Rubinstein, M., *Macromolecules*, **2005**, *38*, 5330.

¹⁸ For unimers and small aggregates a small compression term could rather be taken into account, which is neglected.

¹⁹ Duplantier, B. *J. Stat. Phys.* **1989**, *54*, 581-680.

²⁰ Hsu H.-P., Nadler W., Grassberger P., *Macromolecules*, **2004**, *37*, 4658-4663.

²¹ Daoud, M.; Cotton, J. P. *J. Phys. (France)* **1982**, *43*, 531.

²² Nyrkova I. A., Semenov A. N., *Eur. Phys. J. E*, **2005**, *17*, 327-337.

²³ This loose definition of the *CMC* does not exactly coincide with the *operational* one detecting the kink in the $\mu(\phi)$ curve discussed previously.

²⁴ This is based on the fact that the stretching energy of the corona and the surface tension of the core are comparable at the *CMC* and at the maximum of the barrier.

²⁵ Zhulina E. B., Borisov, O. V. , *Macromolecules*, **2002**, *35*, 9191.

²⁶ Currie, E. P. K.; Cohen-Stuart, M. A.; Borisov, O. V. *Macromolecules* **2000**, *34*, 1018.